Journal of Advanced Research 36 (2022) 187–199

Contents lists available at ScienceDirect

Journal of Advanced Research

journal homepage: www.elsevier.com/locate/jare

Coordination of root growth with root morphology, physiology and defense functions in response to root pruning in *Platycladus orientalis*

Zhipei Feng [a,1], Deliang Kong [a,1], Yuhua Kong [a], Baohong Zhang [b], Xitian Yang [a,*]

[a] College of Forestry, Henan Agricultural University, Zhengzhou, Henan 450002, China
[b] Department of Biology, East Carolina University, Greenville, NC 27858, United States

HIGHLIGHTS

- A growthdefense tradeoff following root pruning.
- Root growth lagged behind root physiology after root pruning.
- The growthdefense tradeoff was induced by indole-3-acetic acid.
- Proteomic analysis supported a growthdefense tradeoff.
- Root pruning altered the expression of genes at the protein and mRNA levels.

GRAPHICAL ABSTRACT

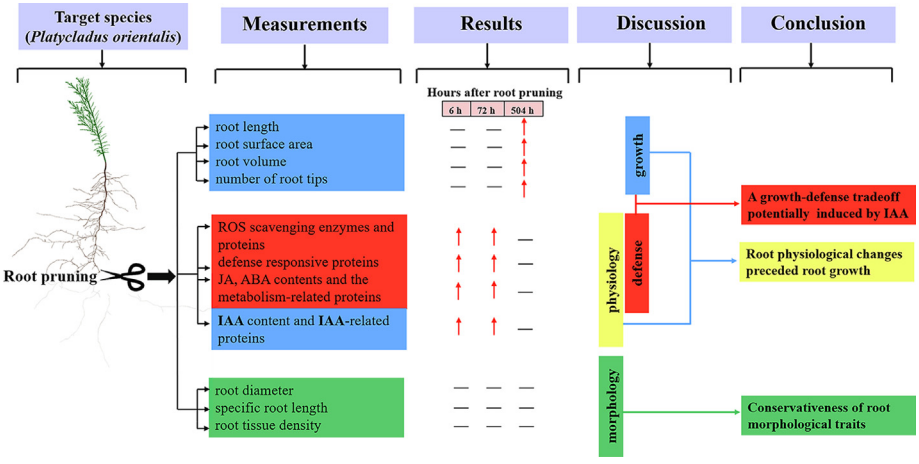

ARTICLE INFO

Article history:
Received 24 October 2020
Revised 23 June 2021
Accepted 8 July 2021
Available online 14 July 2021

Keywords:
Root pruning
Root growth
Root morphology
Root physiology
Growth-defense tradeoff
Platycladus orientalis

ABSTRACT

Introduction: Root pruning is commonly used to facilitate seedling transplantation for the restoration of degraded or damaged ecosystems. However, little is known about how root growth coordinates morphology, physiology and defense functions following root pruning.
Objectives: We aim to elucidate whether and how root growth trades off with defense functioning after pruning.
Methods: Seedlings of *Platycladus orientalis*, a tree species widely used in forest restoration, were subjected to root pruning treatment. A suite of root growth, morphological and physiological traits were measured after pruning in combination with proteomic analysis.
Results: Root growth was insensitive to pruning until at 504 h with a significant increase of 16.8%, whereas root physiology was activated rapidly after pruning. Key root morphological traits, such as root diameter, specific root length and root tissue density, showed no response to the pruning treatment. Plant defense syndromes such as reactive oxygen species-scavenging enzymes and defensive phytohormones such as jasmonic acid and abscisic acid, were recruited at six hours after pruning and recovered to the unpruned levels at 504 h. Compared with the controls, 271, 360 and 106 proteins were differentially

Peer review under responsibility of Cairo University.

* Corresponding author.
E-mail address: yangxt@henau.edu.cn (X. Yang).

[1] These authors contributed equally.

https://doi.org/10.1016/j.jare.2021.07.005

expressed at 6, 72 and 504 h after root pruning, respectively. These proteins, associated with defense function, showed temporal patterns similar to the above defense syndromes.
Conclusion: Our results suggest a root growth-defense tradeoff following root pruning in *P. orientalis*. This tradeoff was potentially due to the significant increase of indole-3-acetic acid, the phytohormone stimulating root branching, which occurred soon after pruning. Together, these results provide a holistic understanding of how root growth is coordinated with root morphology, physiology, and defense in response to root pruning.

Introduction

Afforestation is an effective method adopted worldwide for forest restoration, especially in degraded and damaged ecosystems [1,2]. Root pruning is usually performed to facilitate the transplantation and transportation of tree seedlings. However, root pruning can cause the seedlings to suffer great root tissue loss and damage, and as such, can result in adverse effects on nutrient foraging and seedling growth and survival [3,4]. Given the crucial role of roots in plant nutrient acquisition, it is of great importance to assess the effects and underlying mechanisms of pruning on root growth and functioning.

Significant shifts in root growth, morphology and physiology have been frequently observed after root pruning [5–7]. For example, following root pruning, lateral root growth is greatly enhanced in *Platycladus orientalis* seedlings [6]. Compensatory increases in the specific root length, fine root vitality and the ratio of fine roots to the total root mass have been reported in *Cunninghamia lanceolata* [5]. Meanwhile, roots are among the primary agents in plants for sensing and responding to environmental signals [8,9]. A conspicuous phenomenon is that root pruning could induce significant changes in the contents of phytohormones, such as increases in the contents of indole-3-acetic acid (IAA), jasmonic acid (JA) and abscisic acid (ABA) in roots, which are usually involved in plant growth and defense responses [8–11]. Moreover, under stress or disturbance conditions, such as root pruning, the plant antioxidative enzyme system is activated to clear the excessive reactive oxygen species (ROS) [12–14]. Antioxidative enzymes employed by plants usually include peroxidase (POD), superoxide dismutase (SOD), glutathione-S-transferase (GST) and catalase (CAT). Eventually, changes in the contents and activities of phytohormones and enzymes jointly contribute to the recovery of the pruned roots or to the initiation of lateral roots following pruning [9,10,13]. However, most previous studies have mainly focused on one or few traits associated with root growth, morphology and physiology; the traits are also usually measured only once after root pruning.

It is increasingly recognized that root growth, morphology and physiology respond asynchronously to environmental changes [15–18]. For example, root nitrogen content and respiration are much more sensitive to soil nutrient enrichment than root diameter and tissue density [16,19]. Therefore, it is pivotal to account for root growth, morphology and physiology to obtain a holistic understanding of the responses of plant roots to pruning treatment over time. Furthermore, plant roots are usually faced with a growth-defense tradeoff, especially under stress or disturbance conditions [20–23]. Little is known about how roots respond to disturbance, such as root pruning, by coordinating their growth and defense functions over time.

Proteomics is emerging as a powerful tool for shedding light on the molecular mechanisms underlying root responses to environmental changes [24,25]. For example, compared with the responses of *Arabidopsis thaliana* roots to nitrate, their responses to ammonium can be potentially attributed to a set of differentially expressed proteins in the roots [26]. Proteins related to osmotic adjustment, ion homeostasis and antioxidative defense play crucial roles in root adaption to salt stress in *Hordeum spontaneum* [27] and to water limitation in *Quercus ilex* [24]. Similarly, the expression of proteins associated with carbohydrate metabolism and phytohormones in the roots of *Populus cathayana* could be responsible for plant adaption to nitrogen deficiency [28]. It is likely that root responses to pruning could be associated with different profiles of proteins involved in ROS cleavage and phytohormone pathways. However, to date, few studies have employed proteomics to reveal the mechanisms underlying physiological, growth and morphological changes that occur in the roots over time after pruning treatment.

Platycladus orientalis is widely planted in afforestation projects in northern China due to its ecological and commercial importance [29,30]. However, root loss and damage induced by root pruning greatly affect the growth, survival and productivity of planted *P. orientalis* forests [29,31]. To fully understand the responses of *P. orientalis* roots to pruning, changes in root growth, morphology and physiology and in the root proteomes of pruned and unpruned seedlings were investigated at different time points following pruning. Specifically, the following hypotheses were tested: (1) the responses of root physiology to root pruning decline with time, whereas root growth and morphology show greater responses after longer periods of time after pruning; and (2) there is a tradeoff between root growth and defense with time following the pruning treatment, that is, soon after pruning, roots prefer to recruit defense function, while after longer periods of time, roots invest more in growth than in defense.

Materials and methods

Study site

The experiment was carried out in a greenhouse at the Forestry Ecological Experimental Station of Henan Agricultural University (34°43′N, 113°42′E), Zhengzhou, Henan, China. During the experimental period, the average temperature ranged from 20 °C (night) to 30 °C (day), the relative humidity ranged from 50% (day) to 65% (night), and the light/dark cycle was 14/10 h.

Plant material and experimental design

Seeds of *P. orientalis* were collected from the Yellow River Xiaolangdi Forest Experimental Station (34°58′−35°07′N, 112°23′−112°32′E), Jiyuan, Henan, China. After harvest, the seeds were stored at 4 °C. The seeds were first sterilized according to our previous study [32]. Then, these seeds were germinated in Petri dishes (25 cm diameter) with sterilized moist filter paper in an incubator at 25 °C/18 °C (day/night) in darkness for 18 days. Uniformly germinated seeds were sown in plastic pots (30 cm × 40 cm × 40 cm; approximately 38 L) with three seeds per pot. The pots were filled with a mixture of organic soil, sand, vermiculite and perlite (2:4:3:1). The pH was 8.02. The contents of available nitrogen, phosphorus and potassium in the growth substrate were 67.77, 27.56 and 55.12 mg kg^{-1}, respectively, and

the organic matter content was 6.65 g kg^{-1}. After seedling emergence, only one seedling was retained in each pot. All seedlings were watered once every three days (1000 mL per pot) over the course of the growth period. All pots were placed on circular trays and randomly rearranged at 3-day intervals to minimize the effects of heterogeneity of the microenvironments. After six months, 360 uniformly healthy seedlings (height of 96.32 ± 2.73 mm and ground diameter of 1.04 ± 0.21 mm) were selected for the experiment. Among them, the roots of 180 seedlings were pruned according to our previously described procedures [6,11]. In brief, the 360 seedlings were all carefully removed from the pots and half (180 seedlings) had their taproots pruned and the other half did not. For the pruning treatment, a medium level of root pruning was used; the bottom third of the taproot (by length) was removed, after which plants have been shown to display the highest growth potential [6]. After root pruning, both the pruned and unpruned seedlings were replanted in the original 38-L pots.

Root sampling

Sixty individual seedlings were harvested from both the pruned and unpruned groups at 6, 72 and 504 h after the treatment. The three sampling time points were determined by the time of the maximum antioxidative enzyme (e.g., POD and SOD) activities (i.e., six hours), the emergence of new lateral root apices (i.e., 72 h) and the stabilizing of the difference in root growth between pruned and unpruned roots (i.e., 504 h), respectively. The new lateral root apices could be easily identified by their color and texture, and these apices would eventually develop into mature lateral roots. To harvest the roots from the pots, the aboveground parts of each seedling were first cut off, and then the plastic pots were tenderly destroyed. The whole root systems were carefully separated from the soil, gently washed with tap water, and then rinsed with distilled water. Half of the root samples were stored at 4 °C for root growth and morphological measurements. The other half of the root samples were immediately frozen in liquid nitrogen, and then stored at − 80 °C in preparation for the physiological and proteomic analyses. At each measurement, 10 roots from each treatment group (pruned and unpruned) were randomly selected and mixed as a composite sample forming one biological replicate. Therefore, there were three biological replicates, each including 10 roots, for the measurements of root growth, morphology and physiology and real-time quantitative reverse transcription polymerase chain reaction (qRT-PCR) analysis. For the proteome analyses we used two biological replicates, as done in other studies [33,34].

Root growth and morphology

The roots were scanned using an Epson Perfection V700 Photo scanner (Epson Company, Ltd., Japan). Root length, root surface area, root volume, number of root tips and root diameter were analyzed using WinRhizo Pro 2007d software (Regent Instruments, Canada). After root scanning, the root length per tip was estimated as the ratio of root length to the number of root tips. Roots were oven-dried at 75 °C for 72 h and weighed. Specific root length and root tissue density were estimated as the ratios of root length to root dry mass and root dry mass to root volume, respectively. All root diameters were much<1 mm, and thus, the roots could be considered as absorptive roots [35]. Root growth was expressed as the root biomass, length, surface area, volume and number of root tips at each sampling time.

Determination of antioxidant enzyme activities

Fresh roots (0.5 g) were added to 1% (w/v) polyvinylpolypyrrolidone and ground into a fine powder in liquid nitrogen. Then, the powder was homogenized in an extraction buffer containing 50 mM K_2HPO_4 buffer (pH 7.8), 0.1 mM phenylmethanesulfonyl fluoride, 1 mM disodium ethylenediaminetetraacetic acid, and 0.3% (v/v) Triton X-100 in ice-cold mortars. The resulting solution was subjected to centrifugation at 12,000 × *g* for 20 min at 4 °C. The supernatant was collected and used for further measurement of enzyme activity. POD and SOD activities were measured using the POD and SOD assay kits (Nanjing Jiancheng Bioengineering Institute, China) according to the protocols of the manufacturer and were expressed as units mg^{-1} protein.

Quantification of JA, ABA and IAA contents

Approximately 0.5 g of roots from pruned and unpruned *P.orientalis* at 6, 72 and 504 h after pruning were ground in liquid nitrogen. The JA, ABA and IAA contents were quantified using the enzyme-linked immunosorbent assay kits of JA, ABA and IAA (China Agricultural University, China) following the respective protocols.

Protein extraction

Total proteins were extracted from the roots of pruned and unpruned *P. orientalis* seedlings using a cold trichloroacetic acid-acetone method according to the methods described in a previous study [36] with minor modifications. Briefly, a total of 1000 mg of frozen root tissue from each sample was ground into a fine powder with 100 mg of 1% (w/v) polyvinylpolypyrrolidone in liquid nitrogen. The entire mixture was transferred into an Eppendorf microcentrifuge tube with one volume of 10% (w/v) trichloroacetic acid and nine volumes of ice-cold acetone. This mixture was vortexed for 30 s, and then stored overnight at − 20 °C. Combined homogenates were centrifuged at 30,000 × *g* for 30 min at 4 °C. The resulting supernatants were discarded, and the precipitates were collected. Precipitated proteins were suspended with pre-cooled acetone three times and recentrifuged at 20,000 × *g* for 30 min at 4 °C. The protein pellet of each sample was dried for 5 min using a vacuum concentrator (Eppendorf, USA) and was resuspended with STD buffer containing 4% (w/v) sodium dodecyl sulfate, 100 mM Tris-HCl (pH 8.0) and 1 mM dithiothreitol. The suspensions were incubated in a boiling water bath for 5 min, followed by 10 s ultrasonication for 10 times, and then placed in a water bath for 15 min. The liquid mixture was centrifuged again at 20,000 × *g* for 30 min at 4 °C and the final supernatants were collected. Protein concentrations were quantitated using a bicinchoninic acid protein assay kit (Thermo Pierce, Rockford, IL, USA).

Sodium dodecyl sulfate polyacrylamide gel electrophoresis (SDS-PAGE)

The proteins (20 μg) that were extracted from the pruned and unpruned roots at each time point following root pruning, were diluted in loading buffer. The loading buffer consisted of 10% (w/v) SDS, 50% (v/v) glycerol, 0.5% (w/v) bromophenol blue, 500 mM dithiothreitol and 250 mM Tris-HCl (pH 6.8). Subsequently, the reaction mixtures were incubated in a boiling water bath for 5 min. Protein quality was detected using 12.5% SDS-PAGE, staining with a solution of Coomassie Brilliant Blue R-250 for 2 h, destaining with a destaining solution (10% methanol and 7% acetic acid) for 30 min, and washing three times with ultrapure water.

Protein digestion and isobaric tags for relative and absolute quantitation (iTRAQ) labeling

The extracted protein (100 μg) from each sample was dissolved in 30 μL of STD buffer. Subsequently, samples were placed in a water bath for 15 min and then cooled to room temperature. After

mixing with UA buffer (8 M urea and 150 mM Tris-HCl [pH 8.0]), samples were transferred into a 10 kDa molecular weight cut-off centrifugal filter (Millipore Corp., Billerica, MA, USA) for repeated ultrafiltration. The collected filtrates were centrifuged at 14,000 × *g* for 15 min at 4 °C. Then, 200 μL of UA buffer was added followed by centrifugation under the same conditions. An additional 100 μL of iodoacetamide in UA buffer was added to the protein reactions, which were placed in the dark for 30 min and centrifuged again. The filters were washed three times using UA buffer. Subsequently, 100 μL of DS buffer (50 mM triethylammonium bicarbonate [pH 8.5]) was added, followed by centrifugation as described above. This process was repeated twice. The suspension from each sample was then digested overnight using 40 μL of trypsin (Promega, Madison, WI, USA) in 40 μL of DS buffer at 37 °C. Following digestion, peptides of each sample were eluted with C18 desalting cartridges (Empore™ standard density SPE C18 Cartridges; bed I.D. 7 mm, 3 mL volume; Sigma, St. Louis, MO, USA), concentrated under vacuum and resuspended in 40 μL of 0.1% (v/v) formic acid. Peptide contents were determined by ultra-violet light spectral density at a wavelength of 214 nm.

The extracted peptides (100 μg) from each sample were labeled using the iTRAQ reagents 8-plex multiplex kit (AB Sciex, Framingham, MA, USA) according to the methods of a previous study [37]. The resulting peptides from the pruned and unpruned root samples at the three sampling times (6, 72 and 504 h after root pruning) were labeled using different iTRAQ tags (113, 114, 115, 116, 117 and 118), following the manufacturer's instructions. Two replicates were performed independently. The iTRAQ workflow chart is shown in Fig. 1.

Strong cation exchange (SCX) chromatography fractionation

Twelve labeled peptide extracts were fractionated by SCX using an ÄKTA purifier system (GE Healthcare, Piscataway, NJ, USA). Each sample was dried in a vacuum centrifuge and reconstituted with solvent A (10 mM KH_2PO_4 in 25% [v/v] acetonitrile, pH 3.0). The resulting sample was then loaded onto a Polysulfoethyl A column (PolyLC Inc., Columbia, Maryland, USA) with a 4.6-mm inner diameter and length of 100 mm. The resulting peptides were first eluted at a 1 mL min^{-1} flow rate with a step gradient as follows: solvent A for 40 min, 0% solvent B (500 mM KCl, 10 mM KH_2PO_4 in 25% [v/v] acetonitrile, pH 3.0) for 25 min, 0–10% solvent B for 7 min, 10%–20% solvent B for 10 min, 20%–45% solvent B for 5 min, 45%–100% solvent B for 5 min, and 100% solvent B for 8 min. The resulting eluent was monitored by checking the absorbance at 214 nm. Fractions were collected at 1 min, dried in a vacuum centrifuge, and dissolved with 0.1% (v/v) trifluoroacetic acid. Fraction collections were desalted with SPE C18 Cartridges (Empore™ standard density C18 cartridges; bed I.D. 7 mm, 3 mL volume; Sigma, St. Louis, MO, USA), lyophilized, and redissolved in buffer A (0.1% [v/v] formic acid in water).

Liquid chromatography with tandem mass spectrometry (LC-MS/MS) analysis

LC-MS/MS analysis of the samples was performed using an Easy nLC Nano-HPLC system (Thermo Fisher Scientific, Waltham, MA, USA) combined with a Q-Exactive mass spectrometer system (Thermo Finnigan, San Jose, CA, USA). The resulting peptide mixture was injected into a Nano-HPLC-Easy nLC system equipped with Thermo Scientific Easy columns in buffer A. Subsequently, separation was performed with a linear gradient of buffer B (0.1% [v/v] formic acid and 84% [v/v] acetonitrile) flowing at 300 nL min^{-1}. The elution gradient of buffer B from 0% to 90% was as follows: 0–10% for 2 min, 10%–45% for 46 min, 45%–90% for 5 min, and finally 90% for 10 min. Chromatographic conditions were maintained at 5% buffer B for 5 min followed by equilibration with 5% buffer B for 15 min. The Q-Exactive mass spectrometer system was used in positive ionization mode for data-dependent acquisition of separation samples according to the following parameters: full scan range of 300 < m/z < 1800 at a resolution of 70,000, 40 ms accumulation time per spectrum, high-energy collisional dissociation (HCD) spectra at a resolution of 17,500, automatic gain control target for 1e6, and dynamic exclusion duration for 60.0 s. The mass spectrometry proteomics data have been deposited in the ProteomeXchange Consortium (http://proteomecentral.proteomexchange.org) via the Proteomics Identifications Database partner repository with the dataset identifier PXD020698.

Sequence database search and data analysis

All the HCD-generated MS/MS spectra were analyzed using Mascot (version 2.3.02; Matrix Science, London, UK) embedded in Proteome Discoverer (version 2.1; Thermo Scientific, San Jose, CA) and a search was performed against our transcriptomic database of *P. orientalis* (SRR12349536; https://www.ncbi.nlm.nih.gov/sra/PRJNA649657). The search criteria are shown in Table S1. Quantitative comparisons of pruned and unpruned root samples at each time point were performed taking into account only statistically significant changes based on Student's *t*-tests at $P < 0.05$. Differentially expressed proteins between the pruning and non-pruning treatments were assessed according to the threshold criteria of ≥ 1.20-fold or ≤ 0.83-fold change with $P < 0.05$ for the protein quantities [38,39] in *P. orientalis* roots. Hierarchical clustering was performed for the relative expression ratios of differentially expressed proteins in the roots between pruned and unpruned seedlings at the three time points using R software.

Bioinformatics analysis

The identified proteins were classified into three functional categories: biological process, molecular function and cellular component, according to the Gene Ontology (GO) database (http://www.geneontology.org). Following functional annotation, the metabolic pathways of these identified proteins were mapped according to the Kyoto Encyclopedia of Genes and Genomes (KEGG; http://www.genome.jp/kegg/). Fisher's exact test was employed to test the enrichment of the differentially expressed proteins at each time point against all identified proteins. A GO term or pathway with a *P*-value of<0.05 was considered to be significantly enriched.

RNA extraction and qRT-PCR analysis

Total RNA was isolated from root tissues of pruned and unpruned seedlings using the Plant RNA Extraction Kit (Omega - Bio-Tek, Norcross, GA, USA) in accordance with the manufacturer's recommended protocol. The RNA purity of each sample was measured using a NanoDrop 2000 Spectrophotometer (Thermo Fisher Scientific, Inc., Wilmington, DE, USA). The RNA quality was checked using 1.5% non-denaturing agarose gel electrophoresis. Total RNA (1 μg) was reverse transcribed using the PrimeScript® RT reagent Kit (Takara, Dalian, China) in a 20 μL volume according to the manufacturer's specifications. The qRT-PCR analysis was performed using a Light Cycler® 96 (Roche Diagnostics, Basel, Switzerland) with universal SYBR Green Supermix (Roche, Basel, Switzerland). The PCR amplification was carried out using the following cycling steps: initial denaturation at 95 °C for 3 min, followed by 45 cycles of 95 °C for 10 s and 60 °C for 30 s, and then melting curve analysis at 95 °C for 15 s, 60 °C for 60 s and 95 °C for 15 s. Three technical and three biological replicates were run for pruned and unpruned samples at each time point. Ubiquitin-conjugating enzyme E2 of *P.*

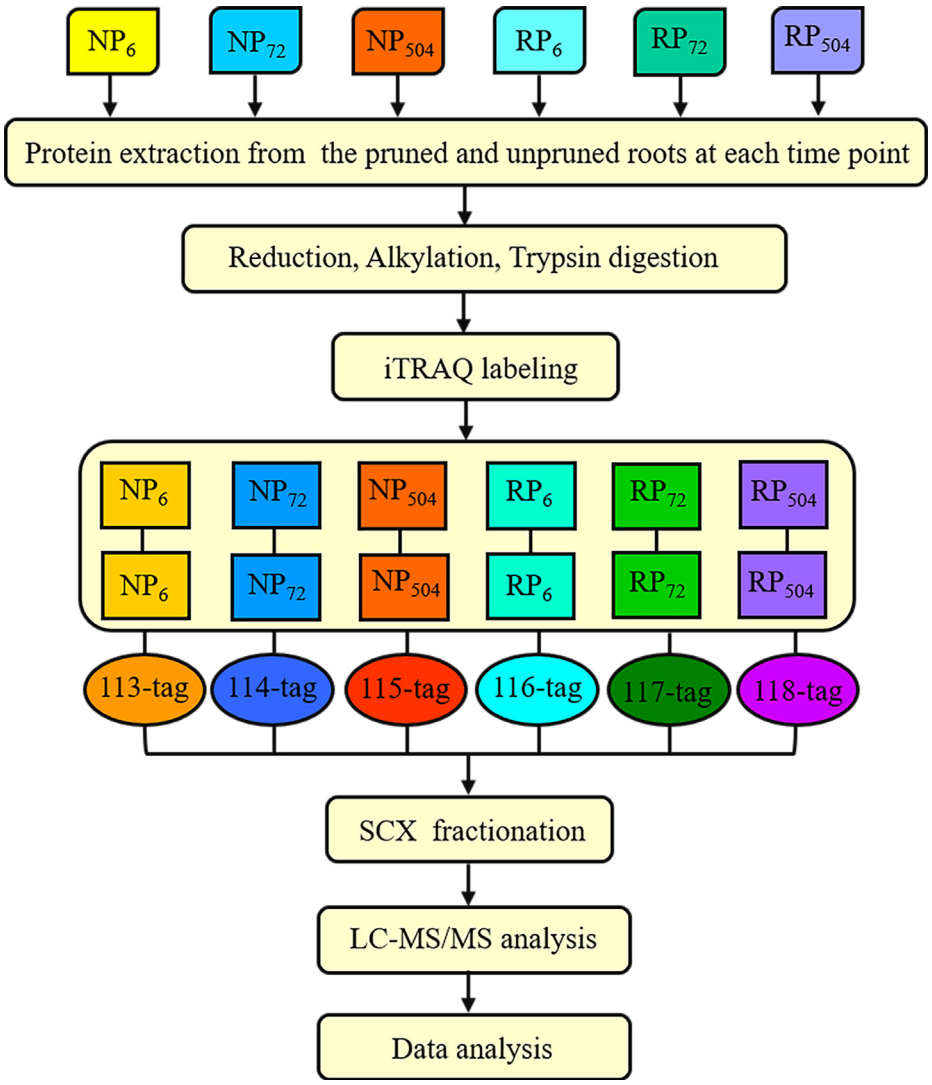

Fig. 1. Schematic diagram for protein identification of pruned and unpruned roots of *P. orientalis* at 6, 72 and 504 h after root pruning using the iTRAQ method. RP, root pruning; NP, non-root pruning. The numerical subscript in the figure shows the hours after pruning. iTRAQ, SCX and LC-MS/MS are the abbreviations for isobaric tags for relative and absolute quantitation, strong cation exchange, and liquid chromatography with tandem mass spectrometry, respectively.

orientalis was used as a reference gene for the normalization of gene expression [40]. Relative gene expression was calculated according to the $2^{-\Delta\Delta Ct}$ method [41], where $\Delta Ct = (Ct_{target\ gene} - Ct_{reference\ gene})$ and $\Delta\Delta Ct = (Ct_{pruned} - Ct_{unpruned})$. Primers used in gene expression analysis were designed using Primer Premier 6.0 software (Premier Biosoft International, Palo Alto, CA, USA) and the sequences are shown in Table S2. The genes analyzed in the qRT-PCR were selected according to the results of the differentially expressed proteins and their annotated functions.

Data analysis

The statistical differences in the root growth, morphological and physiological traits between the pruned and unpruned roots at each sampling time were analyzed using Tukey's test at the $P < 0.05$ level in the SPSS statistical package (version 25.0; IBM Inc., Chicago, IL, USA). If necessary, data were transformed to meet the requirements of normal distribution and equal variance in the analyses.

Results

Responses of root growth and morphology to root pruning over time

At 6 and 504 h after root pruning, no lateral root apices were found in either pruned or unpruned *P. orientalis* (Fig. 2a, 2c, 2d and 2f). In contrast, at 72 h after pruning, approximately seven lateral root apices per root branch were observed for the pruned roots, which was more than six times the amount observed for the unpruned roots ($P < 0.05$, Fig. 2b and 2e). The root pruning treatment significantly increased the root growth of *P. orientalis* only at 504 h after pruning ($P < 0.05$, Fig. 3a–3e). Meanwhile, root pruning had no effects on root length per tip (Fig. 3f) and the three morphological traits (root diameter, specific root length and root tissue density) (Fig. 3 g–3i).

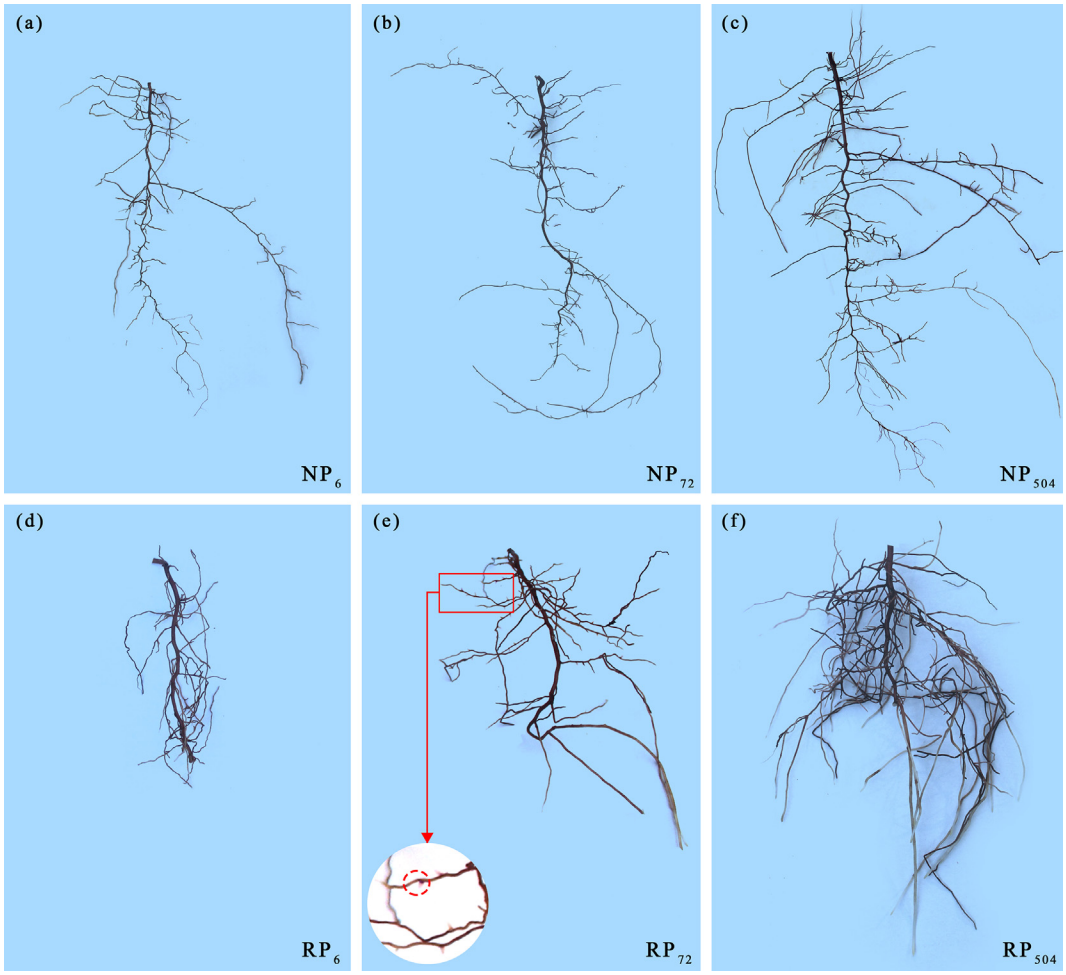

Fig. 2. Roots of *P. orientalis* seedlings between root pruning and non-root pruning treatments at 6 (a and d), 72 (b and e) and 504 (c and f) hours, respectively. The insert figure in panel (e) depicts the new lateral root apex (dashed red circle) at 72 h after pruning. RP, root pruning; NP, non-root pruning.

Root responses to root pruning at the physiological level

Root pruning altered the physiological traits, including the antioxidative enzyme activities and phytohormone contents, of *P. orientalis* roots. The magnitude of these effects generally declined from 6 to 504 h after the pruning treatment ($P < 0.05$, Fig. 4). Specifically, at 6 and 72 h after pruning, root POD activity was 109.4% and 76.78% higher, respectively, in the pruned roots than in the unpruned roots ($P < 0.05$, Fig. 4a). The SOD activity was 13.23% and 16.38% higher at 6 and 72 h, respectively ($P < 0.05$, Fig. 4b). Similarly, at 6 and 72 h after pruning, the root JA (1.6 and 1.33 times), ABA (1.15 and 1.18 times) and IAA (1.56 and 1.32 times) contents were all higher in the pruned roots than in the unpruned roots ($P < 0.05$, Fig. 4c–4e). However, 504 h after root pruning, no significant differences in these root physiological traits were observed between the pruned and unpruned *P. orientalis* seedlings.

Characteristics of identified proteins in P. Orientalis roots

Using the iTRAQ labeling and LC-MS/MS approach, 375,724 spectra were detected for *P. orientalis* roots. Among these spectra, 79,547 were matched to known spectra. A total of 28,239 unique peptides and 5,942 proteins were identified by reference to protein libraries (Table S3).

Of all the identified proteins, 4,261 proteins showed quantitative additivity of the two groups (pruned and unpruned) of *P. orientalis* roots. The molecular weights of the identified proteins ranged from 10 to 305 kDa. Among them, 16.86%, 19.19%, 18.29% and 13.73% had molecular weights of 10–20 kDa, 20–30 kDa, 30–40 kDa and 40–50 kDa, respectively (Fig. S1a). The identified peptides were mainly 7–17 amino acids in length, with most having 9–11 amino acids (Fig. S1b). The peptide number of the identified proteins was mainly<20, and the number of identified proteins declined with the increasing peptide number (Fig. S1c). With respect to the peptide sequence coverage, 70.78% of the identified proteins were distributed at 0–20 (Fig. S1d). Among these identified proteins, the unique peptide number of 1,958 proteins was 1; that of 986 proteins was 2; that of 2,894 proteins was 3–20; and that of 104 proteins exceeded 20 (Fig. S1e). In addition, 5,756 proteins had an isoelectric point between 5 and 10 (Fig. S1f).

Differentially expressed proteins in P. Orientalis roots after root pruning

In total, 678 proteins were differentially expressed in *P. orientalis* roots based on a pairwise comparison between pruned and unpruned samples. The construction of a Venn diagram indicated that 271, 360, and 106 proteins were differentially expressed between pruned and unpruned roots at 6, 72 and 504 h, respec-

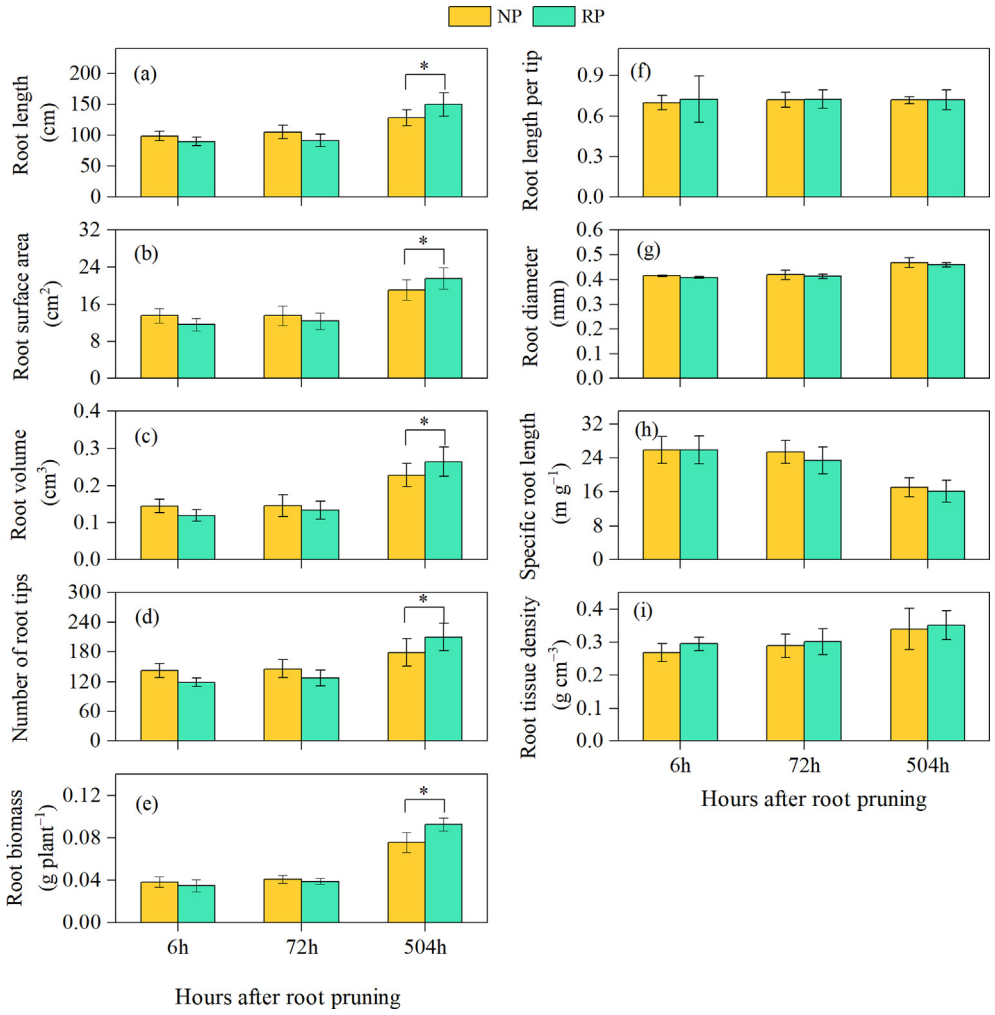

Fig. 3. Changes of root growth and morphology between pruned and unpruned treatments at 6, 72, and 504 h, respectively. Root growth is represented by root length (a), root surface area (b), root volume (c), number of root tips (d), and root biomass (e). Changes of root length per root tip (f) and root morphological traits including root diameter (g), specific root length (h) and root tissue density (i) are shown in the right panels. RP, root pruning; NP, non-root pruning. * represents significant differences ($P < 0.05$) in root investigated traits between the pruned (green bars) and unpruned (yellow bars) treatments at each sampling time. Error bar represents the standard error of three biological replicates.

tively (Fig. 5a). Twenty-eight differentially expressed proteins occurred at both 6 and 72 h following pruning; 17 differentially expressed proteins were found at 72 and 504 h; and 14 differentially expressed proteins were observed at 6 and 504 h (Fig. 5a). Detailed information and fold changes of the differentially expressed proteins are listed in Table S4. Proteins with a significant fold-change of ≥ 1.2 or ≤ 0.83 were regarded as upregulated or downregulated proteins, respectively. More proteins were differentially expressed at 72 h than at 6 and 504 h (Fig. 5b). Among the differentially expressed proteins, 143, 162 and 55 proteins were upregulated, and 128, 198 and 51 were downregulated, at 6, 72 and 504 h, respectively (Fig. 5b). The construction of a heat-map showed the different profiles of the differentially expressed proteins at the three time points (Fig. 5c). Interestingly, the differentially expressed proteins were generally regulated in opposite directions at 6 and 72 h after pruning (Fig. 5c).

Functional analysis of the differentially expressed proteins

Functional annotation using GO revealed that the differentially expressed proteins could be classified into three functional categories, including 16 biological processes, 6 molecular functions and 13 cellular components (Fig. 6). In terms of biological processes, the majority of differentially expressed proteins were mainly involved in metabolic process (GO:0008152), cellular process (GO:0009987), response to stimulus (GO:0050896), localization (GO:0051179), regulation of biological process (GO:0050789), biological regulation (GO:0065007), cellular component organization or biogenesis (GO:0071840) and multi-organism process (GO:0051704). Two differentially expressed proteins (TRINITY_DN14010_c0_g1, TRINITY_DN18629_c0_g1) were assigned to the negative regulation of biological process (GO:0048519) at six hours after root pruning. One differentially expressed protein (TRINITY_DN18447_c0_g11) observed at 72 h following pruning was related to growth (GO:0040007). One differentially expressed protein (TRINITY_DN17530_c0_g2) at 504 h was found to participate in the positive regulation of biological process (GO:0048518). Four GO terms were shared by both pruned and unpruned roots at 72 and 504 h: reproduction (GO:0000003), reproductive process (GO:0022414), multicellular organismal process (GO:0032501) and developmental process (GO:0032502) (Fig. 6a). In terms of the molecular function category, most of the differentially expressed proteins were related to catalytic activity (GO:0003824), binding (GO:0005488), structural molecule activity (GO:0005198), antioxidant activity (GO:0016209) and transporter activity (GO:0005215) (Fig. 6b). For the functional category of cel-

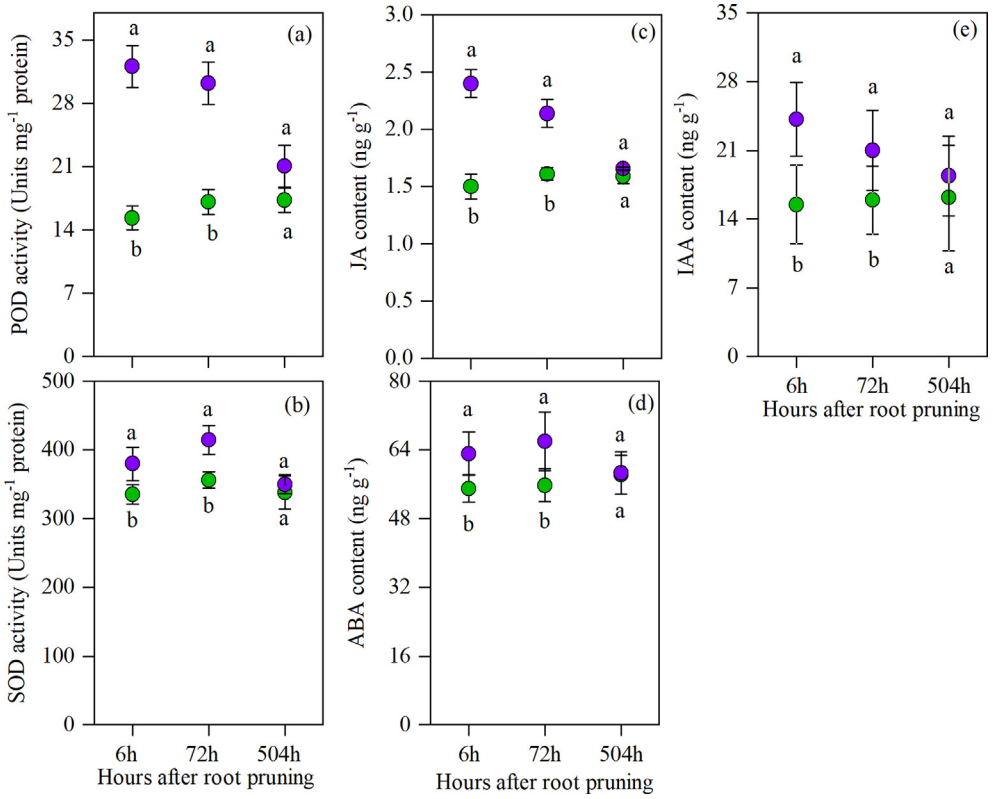

Fig. 4. Changes of antioxidative enzyme activity and phytohormone content between pruned (purple circles) and unpruned (green circles) treatments at 6, 72 and 504 h after root pruning, respectively. Peroxidase (POD) (a) activity, superoxide dismutase (b) activity as well as jasmonic acid (JA) (c), abscisic acid (ABA) (d) and indole-3-acetic acid (IAA) (e) contents of *P. orientalis* roots in both treatments at each sampling time. Different lowercase letters represent statistically significant differences ($P < 0.05$) between the pruned and unpruned roots at each sampling time. Error bar represents the standard error of three biological replicates. RP, root pruning; NP, non-root pruning.

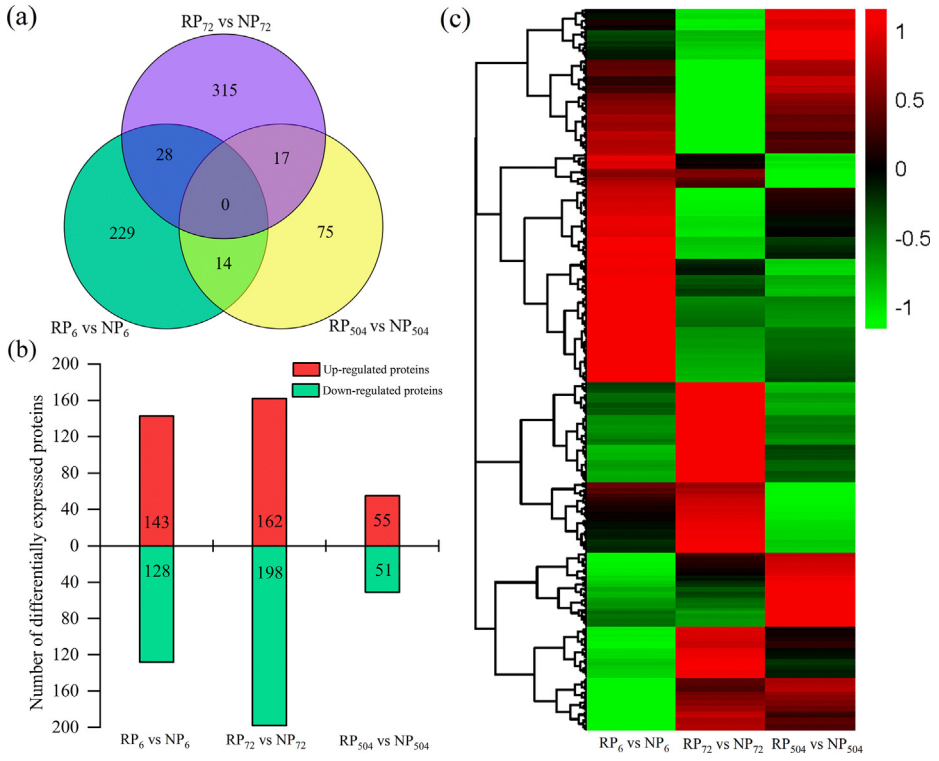

Fig. 5. Comparison of the differentially expressed proteins from *P. orientalis* roots between pruned and unpruned treatments at each sampling time. (a) Venn diagram; (b) the numbers of the upregulated (red bars) and downregulated (green bars) proteins; (c) heat-map for the expression profiles of the differentially expressed proteins. The color scale bar in the right-top corner represents increased (red), decreased (green) and no change (black) of abundance of the proteins, respectively. The sampling time is 6, 72 and 504 h after root pruning as indicated by the numerical subscripts in the figure. RP, root pruning; NP, non-root pruning.

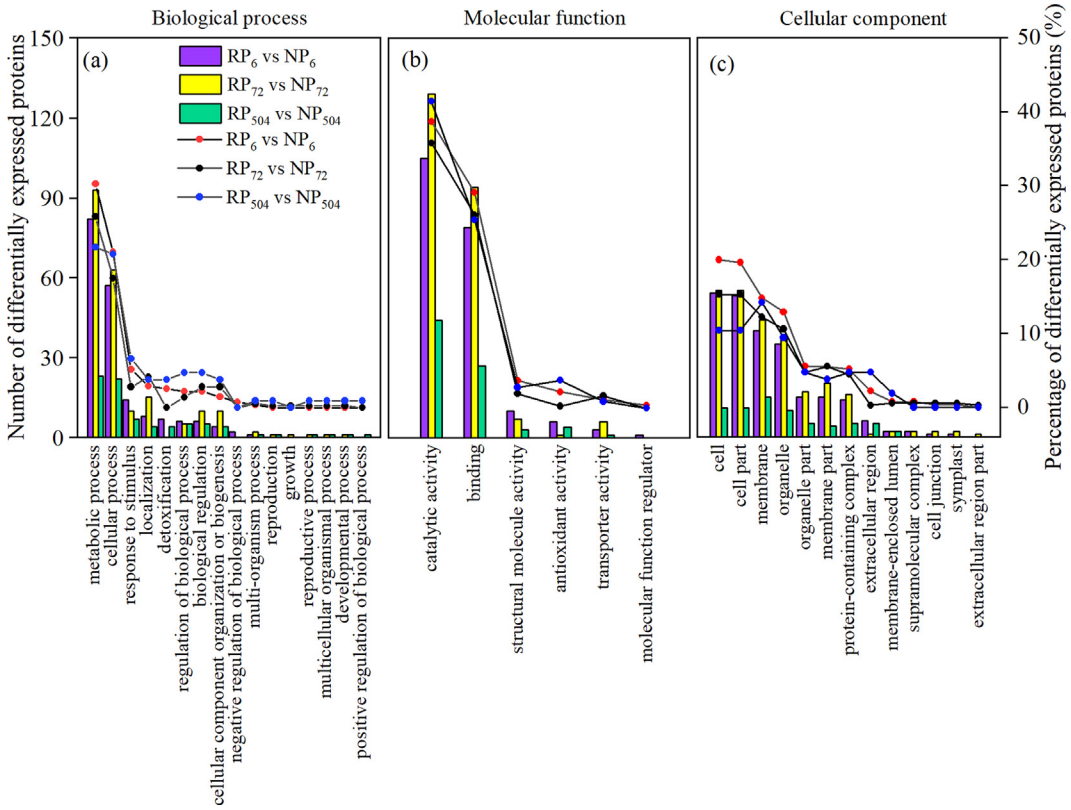

Fig. 6. Differentially expressed proteins based on Gene Ontology (GO) classification for biological process (a), molecular function (b) and cellular component (c) between pruned and unpruned treatments at each sampling time. The purple, yellow and green bars represent numbers of the differentially expressed proteins identified between treatments at 6, 72 and 504 h after root pruning, respectively. The solid black lines with red, black and blue circles indicate the percentage of differentially expressed proteins between treatments, respectively. The sampling time is 6, 72 and 504 h after root pruning as indicated by the numerical subscripts in the figure. RP, root pruning; NP, non-root pruning.

lular component, differentially expressed proteins were mainly associated with cell (GO:0005623), cell part (GO:0044464), membrane (GO:0016020), organelle (GO:0043226), organelle part (GO:0044422) and membrane part (GO:0044425) (Fig. 6c).

To further determine the biological roles of the differentially expressed proteins in the *P. orientalis* roots. GO enrichment analysis was also performed on these proteins at 6, 72 and 504 h after pruning. The results of this analysis showed that 30 GO terms of the biological process category were significantly enriched at six hours following pruning. These terms included hydrogen peroxide catabolic process (GO:0042744, P = 0.0017), hydrogen peroxide metabolic process (GO:0042743, P = 0.0017), response to oxidative stress (GO:0006979, P = 0.0020) and reactive oxygen species metabolic process (GO:0072593, P = 0.0020) (Table S5). Nine GO terms, e.g., defense response (GO:0006952, P = 0.0106), S-adenosylmethionine biosynthetic process (GO:0006556, P = 0.0202) and S-adenosylmethionine metabolic process (GO:0046500, P = 0.0324), were predominantly enriched at 72 h after pruning (Table S5). Significant positive regulation of translational elongation (GO:0045901, P = 0.0354), glucan metabolic process (GO:0044042, P = 0.0400) and pyruvate metabolic process (GO:0006090, P = 0.0443) were observed at 504 h after pruning (Table S5).

Annotation based on KEGG analysis showed that most of the identified differentially expressed proteins were related to ribosome (ko03010), phenylpropanoid biosynthesis (ko00940), glycolysis/gluconeogenesis (ko00010) and α-linolenic acid metabolism (ko00592). KEGG terms such as linoleic acid metabolism (ko00591, P = 0.0117), tyrosine metabolism (ko00350, P = 0.0287) and glucosinolate biosynthesis (ko00966, P = 0.0456), were significantly altered at six hours after pruning. The differentially expressed proteins identified at 72 h after pruning were significantly enriched in valine, leucine, and isoleucine degradation (ko00280, P = 0.0154) and glycine, serine, and threonine metabolism (ko00260, P = 0.0155). The monoterpenoid biosynthesis (ko00902, P = 0.0104) and zeatin biosynthesis (ko00908, P = 0.0178) pathways were predominantly enriched at 504 h following pruning (Table S6).

Transcription and expression profiles of selected proteins

The 11 differentially expressed proteins that were involved in JA pathways (Fig. 7a–7c), ROS scavenging (Fig. 7d and 7e), defense (Fig. 7f–7j) and growth (Fig. 7k), were upregulated or downregulated at both the transcript and protein levels, or were not affected by the pruning treatment. The majority of the protein expression changes after root pruning were similar at mRNA and protein levels, except for some differences possibly caused by post-transcription regulation mechanisms, such as microRNAs.

A proposed model for the integrated responses of roots to pruning

Root pruning could initiate the upregulation of the expression of JA-, ABA- and IAA-related proteins, such as lipoxygenase for JA biosynthesis, ABH1 for ABA signaling pathway and style cell-cycle inhibitor 1 for IAA signaling pathway (Fig. 8①). The JA pathway could also be regulated by Ca^{2+}, ROS signaling and linolenic acid metabolism (Fig. 8①, 8② and 8④). Pruning may impact metabolic processes such as glycolysis, which produces the metabolite, acetyl-CoA. The acetyl-CoA would paticipate in the tricarboxylic

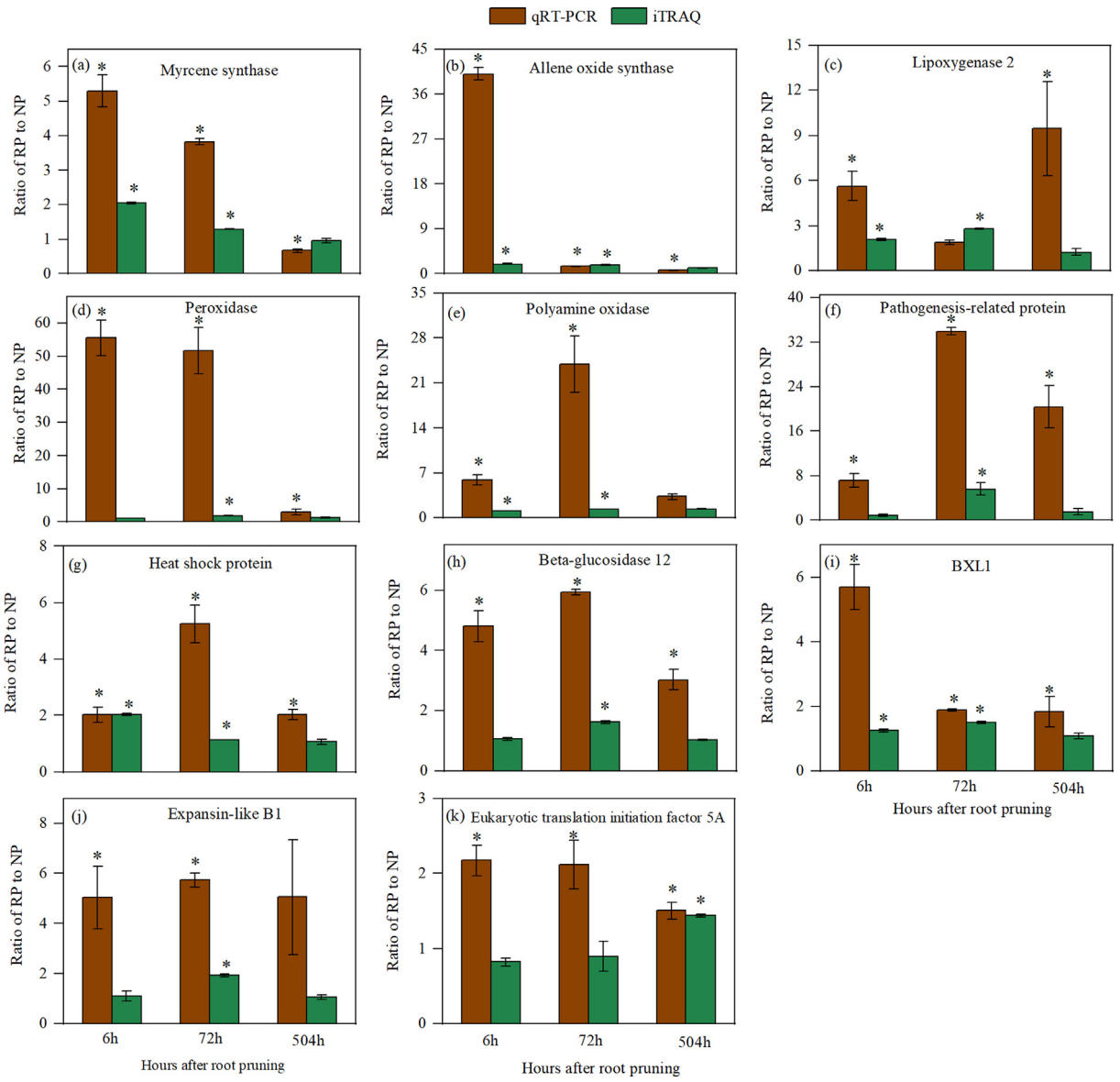

Fig. 7. The ratio of genes (brown bars) and proteins (green bars) between the pruned and unpruned *P. orientalis* roots at 6, 72, and 504 h, respectively. The values indicate mean ± standard error. RP, root pruning; NP, non-root pruning. * represents significance between treatment RP and the control NP at p value < 0.05.

acid cycle to produce NADH and NADPH for the transmembrane transport of ions, ATP or other molecules (Fig. 8② and 8③). Pruning can also cause a surge of ROS, thus initiating ROS scavenging systems such as peroxidase, oxidoreductase and peroxiredoxin (Fig. 8④). Increases in ROS production would also induce the accumulation of defense responsive proteins such as heat shock and pathogenesis-related proteins (Fig. 8⑤). Of these signaling and metabolism pathways, the majority, and especially the defense and ROS-scavenging processes, were regulated at 6 and 72 h after root pruning.

Discussion

Our results clearly show that root pruning can stimulate the root growth of *P. orientalis* only at the late time (504 h) as indicated by the significant increases of root length, surface area, volume and the number of root tips (Fig. 3). Unlike the temporal changes of root growth, prominent changes in root physiology at the biological, molecular and cellular levels occurred in the early time (6 and 72 h) after pruning (Figs. 4 and 6). Therefore, root growth conspicuously lagged behind root physiology in response to root pruning. Interestingly, a prominent occurrence of lateral root apices at the early time (72 h) after root pruning was observed, which contributed mainly to the enhanced root growth at the late time after pruning (Figs. 2 and 3). This suggests that there could be a threshold time over which the accumulation of physiological processes (Fig. 4) will induce visible changes in root growth. Importantly, it was noted that three key root morphological traits, i.e., root diameter, specific root length and root tissue density, which are closely related to root absorptive function [42,43], were not affected by root pruning, irrespective of early and late time after the treatment. This suggests the conservativeness of root morphology in response to root pruning, which contrasts with the great plasticity of root physiology following this treatment. Therefore, these results partially contradict our first hypothesis that predicts greater responses of root morphology at later time after root pruning.

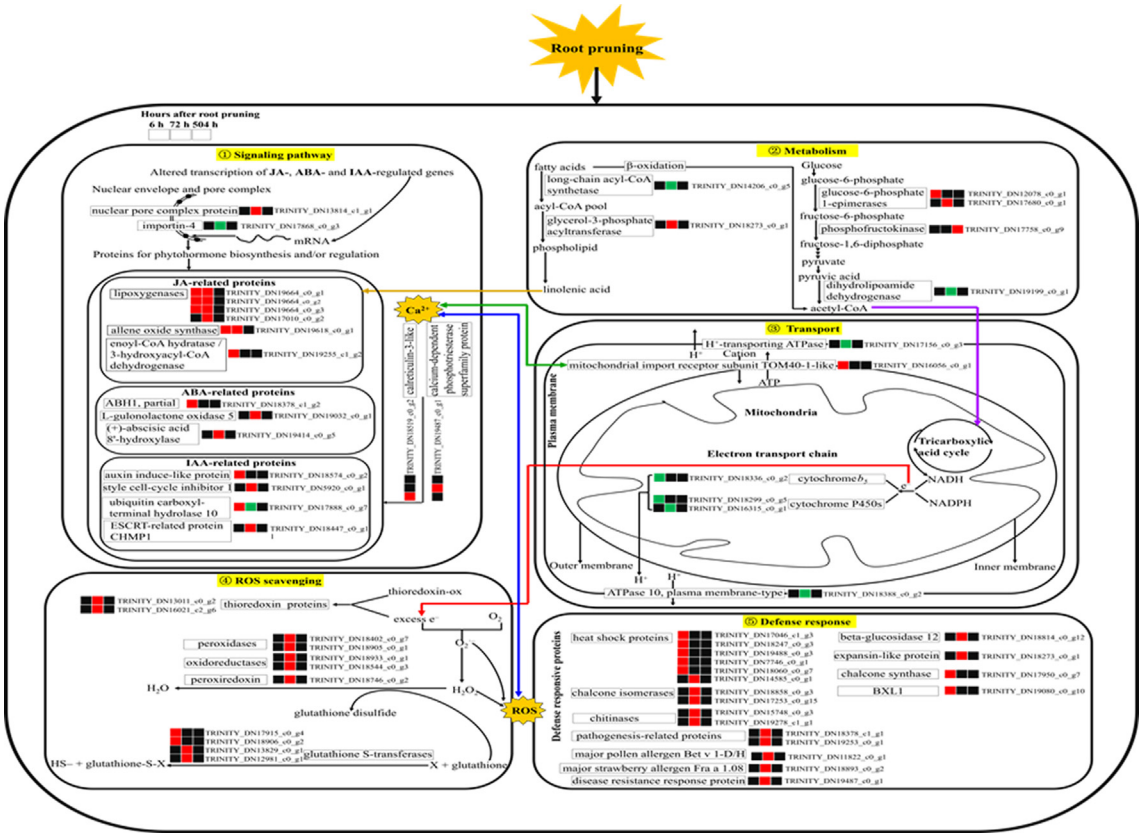

Fig. 8. A conceptual model for *P. orientalis* roots in response to root pruning. The three consecutive squares represent the state of a protein at 6, 72 and 504 h after pruning, respectively, e.g., the squares in red, green and black represent upregulated, downregulated, and no change of the protein. Proteins in red, green and black boxes indicate up-regulated, down-regulated and not-changed by root pruning for *P. orientalis* roots at 6, 72 and 504 h, respectively. Detailed information for the differentially expressed proteins is presented in Table S4.

In accordance with the results of the present study, root morphological traits such as specific root length, also showed no change in response to root pruning in *Quercus robur* [7]. However, several studies have reported significant plasticity of these morphological traits along environmental gradients, such as of climate, soil fertility and moisture [16,17,44–46]. One possible reason for this discrepancy could be that the responses of these root morphological traits to environmental changes are contingent on the identity of the environmental factors. For instance, in infertile soils or cold conditions, roots are usually characterized by a reduction of cell division and greater investment in cell walls, such as via cell wall thickening [42,43]. This will result in considerable changes in root diameter, specific root length and root tissue density. However, in the present study, the soil conditions and microclimate were almost the same for both the pruned and unpruned plants. For *P. orientalis*, a significant increase in root growth was observed with similar root morphology after root pruning (Fig. 3). This suggests that root pruning could have little influence on the investment into root cell walls and hence has only a minor effect on the root morphological traits.

In this study, it was hypothesized that after root pruning, root defense function would be activated first, followed by the initiation of root growth. It is true that root defense syndromes were recruited at the early time following pruning (Figs. 4 and 8). For example, ROS scavenging enzymes, such as POD, SOD, peroxiredoxin, thioredoxin and GST, were significantly activated in pruned *P. orientalis* roots than in unpruned roots at 6 and 72 h after root pruning (also see Figs. 4 and 8). This is mainly caused by a burst of ROS after mechanical injuries such as root pruning [13,47]. Generally, these enzymes are involved in coping with ROS stress; if not cleared effectively, ROS can cause membrane lipid peroxidation or even apoptosis [12–14]. Beside the ROS-induced oxidative stress, pruned roots are inevitably faced with a high risk of pathogen infection, which might induce plant immune responses. Indeed, the results showed that JA- and ABA-related proteins were significantly upregulated (Fig. 8①) as were a suite of key proteins (e.g., heat shock protein, chitinase and pathogensis-related protein; Fig. 8⑤) that function in pathogen defense [24,48–51]. It is also noted that the defense proteins and phytohormones declined after six hours following root pruning. This may be a reflection of strong investment in root growth after the defense function is met.

Interestingly, we also observed that the content of root IAA, which is a key phytohormone stimulating root branching [52,53], increased significantly a few hours after root pruning, and later recovered to the pre-pruned level (Fig. 4). This finding was further supported by the proteomic results; proteins related to IAA were significantly activated in the early time after pruning (Fig. 8①). In addition, a pronounced emergence of lateral root apices was observed in the early time following pruning (Fig. 2). Although no visible changes in root growth were observed in the early time after root pruning (Fig. 3a–3d), a pronounced emergence of lateral root apices was observed at this time (Fig. 2). This suggests that physiological processes triggering root growth in the late time after root pruning were indeed recruited in the early time after root pruning. The early enhanced IAA synthesis results in later root growth and development evidenced by the root length and surface area and total root biomass 504 h after root pruning. It is interesting to note a concomitant change of IAA and defense

phytohormones, such as JA and IAA, immediately following root pruning (Figs. 4 and 8). The activation of IAA in the early time after root pruning could be realized by the crosstalk among the phytohormone pathways [54,55]. After six hours following root pruning, root IAA content declined and recovered to the unpruned level at 504 h. This could be an evolutionarily reasonable result because if the IAA content is still high at 504 h following pruning, the new lateral root apices can be stimulated and hence produce much denser roots. The dense root system could cause strong within-root competition in the limited soil space [56,57], which hinders root resource foraging and could be eliminated by natural selection.

Plants are generally confronted with a tradeoff between growth and defense functioning [22,58,59]. This tradeoff can be more significant under stress or disturbance conditions as plants need to invest more resources into defense, hence reducing the investment in growth [57]. In the present study on *P. orientalis*, root growth remained constant in the early time (e.g., 6 and 72 h) after the pruning treatment but increased significantly in the late time (504 h) (Fig. 3). Root defense function, by contrast, showed a temporally opposing response. For example, defense responsive proteins, defensive phytohormones and antioxidative enzymes were significantly increased in the early time after root pruning, and later returned to unpruned levels (Figs. 4 and 8). These results suggest that there is a temporal tradeoff between growth and defense after root pruning in *P. orientalis*.

Platycladus orientalis is a shallow-rooted tree species and most lateral roots occur in the middle and upper zones of the taproots [31]. Thus, the pruning treatment used in the present study may not greatly reduce the total root length of *P. orientalis*. In this sense, the greater number of root apices (six times higher; Fig. 2) in the early time (72 h) after the pruning treatment could be responsible for the increase in root growth observed at the late time following pruning. This suggests that the root growth-defense tradeoff might result from the higher root growth, which was initiated in the early time after root pruning. Generally, under stress or disturbance conditions, plants preferentially trigger their defense and immune systems [22,58]. In this study, it was found that the physiological mechanisms accounting for the enhanced root growth at the late time after pruning, were initiated quickly in the early time after the pruning occured. Initiation of such physiological mechanisms is usually energy expensive, and is usually expected to occur at a later time following pruning. It is possible that the pruning of *P. orientalis* roots could be a stimulus to reallocate resources stored in taproots (e.g., carbon and nutrients) for lateral root growth [60]. This is an interesting explanation that warrants further investigation, such as investigating the gene functions through the advanced CRISPR/Cas9 genome editing technologies [61,62].

Conclusion

Here, by comprehensively measuring changes of root growth, morphology, physiology and proteomes at different time points following root pruning, we identify a temporal tradeoff between root growth and defense functions following the pruning treatment. The root growth-defense tradeoff could be related to IAA, a key phytohormone stimulating root branching, which could be activated by the crosstalk between IAA and defense phytohormones such as JA and ABA. These results suggest that proper root pruning is an effective way of stimulating root growth and potentially facilitating seedling survival during afforestation. To ensure the practical application of the root pruning, it is necessary to ascertain the effectiveness of this treatment following field transplantation of *P. orientalis*. Furthermore, we may also evaluate the benefit of root pruning for other plant species in northern China in future research.

Compliance with Ethics Requirements

This article does not contain any studies with human or animal subjects.

CRediT authorship contribution statement

ZF: Data curation, Formal analysis, Investigation, Methodology, Validation, Visualization, Writing - original draft, Writing - review & editing. **DK:** Data curation, Formal analysis, Investigation, Writing - original draft, Writing - review & editing. **YK:** Formal analysis, Investigation, Methodology, Writing - review & editing. **BZ:** Formal analysis, Investigation, Methodology, Writing - review & editing. **XY:** Conceptualization, Funding acquisition, Methodology, Project administration, Resources, Software, Supervision, Writing - review & editing.

Declaration of Competing Interest

The authors declare that they have no known competing financial interests or personal relationships that could have appeared to influence the work reported in this paper.

Acknowledgements

We are grateful to the members of 129 laboratory for assistance in field seed collection and laboratory experiments. This study was supported by the National Natural Science Foundation of China (No. 31570613, 31870522) and China Postdoctoral Science Foundation (No. 2021M690922).

Author statement

X.Y. conceived the project and designed the research; Z.F. and Y. K. carried out the experiments; Z.F. and D.K. carried out the data analysis and wrote the manuscript; B.Z. and X.Y. proofread and revised this manuscript.

Appendix A. Supplementary material

Supplementary data to this article can be found online at https://doi.org/10.1016/j.jare.2021.07.005.

References

[1] Peng SS et al. Afforestation in China cools local land surface temperature. PNAS 2014;111(8):2915–9.
[2] Gardner CJ, Struebig MJ, Davies ZG. Conservation must capitalise on climate's moment. Nat Commun 2020;11(1):109.
[3] Andersen L, Rasmussen HN, Brander PE. Regrowth and dry matter allocation in *Quercus robur* (L.) seedlings root pruned prior to transplanting. New For 2000;19(2):205–13.
[4] Benson AR, Morgenroth J, Koeser AK. The effects of root pruning on growth and physiology of two *Acer* species in New Zealand. Urban For Urban Gree 2019;38:64–73.
[5] Dong TF et al. Growth, biomass allocation and photosynthetic responses are related to intensity of root severance and soil moisture conditions in the plantation tree *Cunninghamia lanceolata*. Tree Physiol 2016;36(7):807–17.
[6] Yang XT et al. Effects of different root-cutting treatments on seedling lateral root development. J Henan Agric Univ 2010;44(2):155–9.
[7] Mucha J et al. Functional response of Quercus robur L. to taproot pruning: a 5-year case study. Ann For Sci 2018;75(1):22.
[8] Fanello DD et al. Plasticity of root growth and respiratory activity: root responses to above-ground senescence, fruit removal or partial root pruning in soybean. Plant Sci 2020;290:110296.
[9] Zhou WK et al. A jasmonate signaling network activates root stem cells and promotes regeneration. Cell 2019;177(4):942–56.
[10] Xu DY et al. YUCCA9-mediated auxin biosynthesis and polar auxin transport synergistically regulate regeneration of root systems following root cutting. Plant Cell Physiol 2017;58(10):1710–23.

[11] Yang XT et al. Changes of endogenous phytohormone contents in *Platycladus orientalis* roots after root-cutting. J Henan Agric Univ 2011;45(1):66–70.
[12] Choudhary A, Kumar A, Kaur N. ROS and oxidative burst: Roots in plant development. Plant Diversity 2020;42(1):33–43.
[13] Yang GG et al. Effects of root-cutting on antioxidant enzyme system and osmotic adjustment substances of *Platycladus orientalis*. J Henan Agric Sci 2017;46(7):92–6.
[14] Bais HP et al. Allelopathy and exotic plant invasion: from molecules and genes to species interactions. Science 2003;301(5638):1377–80.
[15] Valverde-Barrantes OJ et al. Fine root morphology is phylogenetically structured, but nitrogen is related to the plant economics spectrum in temperate trees. Funct Ecol 2015;29(6):796–807.
[16] Kramer-Walter KR, Laughlin DC. Root nutrient concentration and biomass allocation are more plastic than morphological traits in response to nutrient limitation. Plant Soil 2017;416(1–2):539–50.
[17] Wang RL et al. Different phylogenetic and environmental controls of first-order root morphological and nutrient traits: evidence of multidimensional root traits. Funct Ecol 2017;32(1):29–39.
[18] Bergmann J et al. The fungal collaboration gradient dominates the root economics space in plants. Sci Adv 2020;6(27):eaba3756.
[19] Roumet C et al. Root structure-function relationships in 74 species: evidence of a root economics spectrum related to carbon economy. New Phytol 2016;210(3):815–26.
[20] Bloom AJ, Chapin III FS, Mooney HA. Resource limitation in plants-an economic analogy. Ann Rev Ecol Syst 1985;16(1):363–92.
[21] Ackerly DD et al. Niche evolution and adaptive radiation: testing the order of trait divergence. J Ecol 2006;87(7):50–61.
[22] Feng YL et al. Evolutionary tradeoffs for nitrogen allocation to photosynthesis versus cell walls in an invasive plant. PNAS 2009;106(6):1853–6.
[23] Huang K et al. Lesser leaf herbivore damage and structural defense and greater nutrient concentrations for invasive alien plants: evidence from 47 pairs of invasive and non-invasive plants. Sci Total Environ 2020;723:137829.
[24] Simova-Stoilova LP et al. Holm oak proteomic response to water limitation at seedling establishment stage reveals specific changes in different plant parts as well as interaction between roots and cotyledons. Plant Sci 2018;276:1–13.
[25] Wang JH et al. Physiological and proteomics analyses reveal the resistance response mechanism to alkali stress in the early seedlings (cotyledons vs. roots) of castor plant (Ricinus communis L.). Environ Exp Bot 2021;185:104414.
[26] Coleto I et al. New insights on *Arabidopsis thaliana* root adaption to ammonium nutrition by the use of a quantitative proteomic approach. Int J Mol Sci 2019;20(4):814.
[27] Shen QF et al. Ionomic, metabolomic and proteomic analyses reveal molecular mechanisms of root adaption to salt stress in Tibetan wild barley. Plant Physiol Biochem 2018;123:319–30.
[28] Song HF et al. Sexually differential gene expressions in poplar roots in response to nitrogen deficiency. Tree Physiol 2019;39(9):1614–29.
[29] Yang XT, Yan DF, Liu CR. Natural regeneration of trees in three types of afforested stands in the Taihang Mountains, China. PLoS ONE 2014;9(9):e108744.
[30] Li BB et al. Severe depletion of available deep soil water induced by revegetation on the arid and semiarid Loess Plateau. For Ecol Manage 2021;491:119156.
[31] Cui QF, Feng ZP, Yang XT. Distributions of fine and coarse tree roots in a semi-arid mountain region and their relationships with soil properties. Trees 2017;31(2):607–16.
[32] Feng ZP et al. Improvements in the root morphology, physiology, and anatomy of *Platycladus orientalis* seedlings from air-root pruning. HortScience 2018;53(12):1750–6.
[33] Zeng X et al. iTRAQ-Based Comparative Proteomic Analysis of the Roots of TWO Winter Turnip Rapes (*Brassica rapa* L.) with Different Freezing-Tolerance. Int J Mol Sci 2018;19(12):4077..
[34] Heng S et al. Cytological and iTRAQ-based quantitative proteomic analyses of *hau* CMS in *Brassica napus* L. J Proteomics 2019;193:230–8.
[35] Guo DL et al. Fine root heterogeneity by branch order: exploring the discrepancy in root turnover estimates between minirhizotron and carbon isotopic methods. New Phytol 2008;177(2):443–56.
[36] Thiellement H et al. Plant proteomics: methods and protocols. Totowa, NJ, USA: Humana Press; 2007. p. 355.
[37] Unwin RD, Griffiths JR, Whetton AD, et al. Simultaneous analysis of relative protein expression levels across multiple samples using iTRAQ isobaric tags with 2D nano LC-MS/MS. Nat Protoc 2010;5(9):1574–82.
[38] Vannini C et al. An interdomain network: the endobacterium of a mycorrhizal fungus promotes antioxidative responses in both fungal and plant hosts. New Phytol 2016;211(1):265–75.
[39] Sun YC et al. Elevated CO_2 increases R gene-dependent resistance of *Medicago truncatula* against the pea aphid by up-regulating a heat shock gene. New Phytol 2018;217(4):1696–711.
[40] Chang EM et al. Selection of reference genes for quantitative gene expression studies in *Platycladus orientalis* (Cupressaceae) using real-time PCR. PLoS ONE 2012;7(3):e33278.
[41] Livak KJ, Schmittgen TD. Analysis of relative gene expression data using real-time quantitative PCR and the $2^{-\Delta\Delta CT}$ method. Methods 2001;25(4):402–8.
[42] Wahl S, Ryser P. Root tissue structure is linked to ecological strategies of grasses. New Phytol 2000;148(3):459–71.
[43] Kong DL et al. Nonlinearity of root trait relationships and the root economics spectrum. Nat Commun 2019;10:2203.
[44] Ding JX et al. Climate and soil nutrients differentially drive multidimensional fine root traits in ectomycorrhizal-dominated alpine coniferous forests. J Ecol 2020;108(6):2544–56.
[45] Kramer-Walter KR et al. Root traits are multidimensional: specific root length is independent from root tissue density and the plant economic spectrum. J Ecol 2016;104(5):1299–310.
[46] Freschet GT et al. Climate, soil and plant functional types as drivers of global fine-root trait variation. J Ecol 2017;105(5):1182–96.
[47] Lew TTS et al. Real-time detection of wound-induced H_2O_2 signalling waves in plants with optical nanosensors. Nat. Plants 2020;6(4):404–15.
[48] Zhao PJ et al. Analysis of different strategies adapted by two cassava cultivars in response to drought stress: ensuring survival or continuing growth. J Exp Bot 2015;66(5):1477–88.
[49] Pavlovic A, Mithoefer A. Jasmonate signalling in carnivorous plants: copycat of plant defence mechanisms. J Exp Bot 2019;70(13):3379–89.
[50] Jia XY et al. Molecular cloning and characterization of wheat calreticulin (CRT) gene involved in drought-stressed responses. J Exp Bot 2008;59(4):739–51.
[51] Sharma A et al. A novel interaction between calreticulin and ubiquitin-like nuclear protein in rice. Plant Cell Physiol 2004;45(6):684–92.
[52] Motte H, Beeckman T. A pHantastic ammonium response. Nat Plants 2020;6(9):1080–1.
[53] Meier M et al. Auxin-mediated root branching is determined by the form of available nitrogen. Nat Plants 2020;6(9):1136–45.
[54] Machado RAR et al. Leaf-herbivore attack reduces carbon reserves and regrowth from the roots via jasmonate and auxin signaling. New Phyto 2013;200(4):1234–46.
[55] Rowe JH et al. Abscisic acid regulates root growth under osmotic stress conditions via an interacting hormonal network with cytokinin, ethylene and auxin. New Phyto 2016;211(1):225–39.
[56] Chen BJW et al. Neighbourhood-dependent root distributions and the consequences on root separation in arid ecosystems. J Ecol 2020;108(4):1635–48.
[57] Colom SM, Baucom RS. Belowground competition favors character convergence but not character displacement in root traits. New Phytol 2021;229(6):3195–207.
[58] Major IT et al. Regulation of growth-defense balance by the JASMONATE ZIM-DOMAIN (JAZ)-MYC transcriptional module. New Phytol 2017;215(4):1533–47.
[59] Li YG et al. DELLA and EDS1 form a feedback regulatory module to fine-tune plant growth-defense tradeoff in *Arabidopsis*. Mol Plant 2019;12(11):1485–98.
[60] Donaldson JR, Kruger EL, Lindroth RL. Competition- and resource-mediated tradeoffs between growth and defensive chemistry in trembling aspen (*Populus tremuloides*). New Phytol 2006;169(3):561–70.
[61] Zhang DQ et al. CRISPR/Cas: A powerful tool for gene function study and crop improvement. Journal of Advanced Research 2021;29:207–21. doi: https://doi.org/10.1016/j.jare.2020.10.003.
[62] Li C et al. CRISPR/Cas: a Nobel Prize award-winning precise genome editing technology for gene therapy and crop improvement. Journal of Zhejiang University-SCIENCE B 2021;22:253–84. doi: https://doi.org/10.1631/jzus.B2100009.